

An analysis of the $t_2 - V$ model

A. Ghosh¹ and S. Yarlagadda^{1,2}

¹ *TCMP Div., Saha Institute of Nuclear Physics, Kolkata, India and*

² *Cavendish Lab, Univ. of Cambridge, Cambridge, UK*

(Dated: August 19, 2021)

We study a model (i.e., the $t_2 - V$ model involving *next-nearest-neighbor hopping* and nearest-neighbor repulsion) in one-dimension that generically depicts the dominant transport mechanism in cooperative strong electron-phonon interaction systems. Using analytic and numerical approaches, hard-core-bosons are shown to typically undergo a striking discontinuous transition from a superfluid to a supersolid. Topological inequivalence of rings with even and odd number of sites is manifested through observable differences (in structure factor peaks) at the transition. Connections are also identified between the $t_2 - V$ model and other topologically interesting models.

PACS numbers: 71.10.Fd, 67.80.kb, 71.45.Lr, 71.38.-k

I. INTRODUCTION

The last few decades have witnessed numerous studies to fathom the tapestry of exotic phenomena (such as long-range orderings) and interesting functionalities (such as colossal magnetoresistance, multiferroicity, superconductivity, etc.)¹ in bulk transition metal oxides (such as the manganites, cuprates, etc.) and their interfaces. Of considerable interest is the coexistence of diagonal long-range orders [such as the charge-density-wave (CDW), spin-density-wave (SDW) and orbital-density-wave (ODW) in manganites²]; also of immense focus is the coexistence and competition between long-range orders that are diagonal (i.e., CDW or SDW) and off-diagonal (i.e., superconductivity or superfluidity) such as those reported in bismuthates³, cuprates⁴, etc.

To model the emergent ordering and functionality in these complex metal oxides (and guide material synthesis), one needs, as building blocks, effective Hamiltonians for various interactions. Except for the cooperative electron-phonon interaction (EPI), effective Hamiltonians, that reasonably mimic the physics, have been derived for all other interactions. For instance, double exchange model approximates infinite Hund's coupling, Gutzwiller approximation or dynamical mean-field theory model Hubbard on-site Coulombic interaction, superexchange describes localized spin interaction at strong on-site repulsion, etc. Many oxides such as cuprates⁵⁻⁷, manganites⁸⁻¹⁰, and bismuthates¹¹ indicate cooperative strong EPI.

Although definite progress has been made long ago in numerically treating EPI systems², only recently has the effective Hamiltonian been derived for the cooperative EPI quantum systems in one-dimension; it has been demonstrated analytically that introducing cooperative effects in the strong EPI limit changes the dominant transport mechanism from one of nearest-neighbor (NN) hopping to that of next-nearest-neighbor (NNN) hopping¹². Additional NN particle repulsion (due to incompatibility of distortions produced by cooperative EPI effects) leads to the $t_2 - V$ model as the effective model.

The purpose of the present paper is to study the $t_2 - V$

model and elucidate the consequences of the atypical dominant (NNN) transport mechanism in cooperative strong EPI systems. We demonstrate that the $t_2 - V$ model, upon tuning repulsion, displays a dramatic discontinuous transition from a superfluid to either a CDW or a supersolid wherein the superfluid and the CDW coexist instead of compete. Green's function analysis yields exact critical repulsion values V_c in the two limiting cases; we find $V_c/t_2 = 4$ for the two hard-core-boson (HCB) case and $V_c/t_2 = 2\sqrt{2}$ for the half-filled system. Using finite size scaling analysis, we also obtain V_c values numerically at intermediate fillings. The symmetry difference between rings with odd number of sites (o-rings) and rings with even number of sites (e-rings) is revealed through the ratio of their structure factor peaks at transition being an irrational number $4/\pi^2$.

The paper is organized as follows. In Sec. II, we present formulae for the structure factor and superfluid fraction (for both $V = 0$ and $V > V_c$) and obtain numerical results for the $t_2 - V$ model in e-rings. Next, in Secs. III and IV, we obtain the exact instability conditions analytically for e-rings at half-filling and for e-rings with two HCBs, respectively. Then for o-rings, in Sec. V, we study numerically the structure factor and superfluid fraction and also derive relevant formulae for them. A comparison is made between e-rings and o-rings in Sec. VI. In Sec. VII, we explain why the Bose-Einstein condensate fraction is zero for our $t_2 - V$ model; in Sec. VIII we discuss the connection between our $t_2 - V$ model and other models. Finally, we discuss our results in Sec. IX and present our conclusions in Sec. X.

II. NUMERICAL STUDY OF THE $t_2 - V$ MODEL FOR e-rings

We begin by identifying the Hamiltonian of the $t_2 - V$ model for HCBs.

$$H_{t_2V} \equiv -t_2 \sum_{j=1}^{N_s} (b_{j-1}^\dagger b_{j+1} + \text{H.c.}) + V \sum_{j=1}^{N_s} n_j n_{j+1}, \quad (1)$$

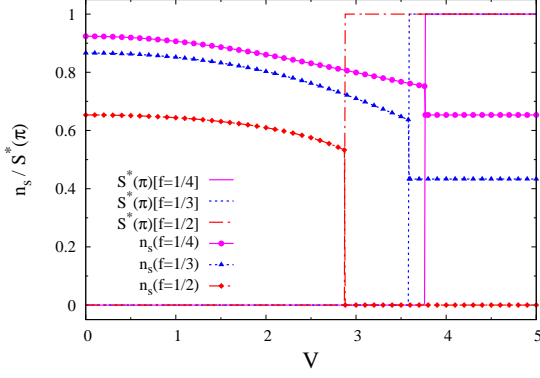


FIG. 1. (Color online) Plots of rescaled structure factor $S^*(\pi)$ and superfluid fraction n_s at various filling factors f obtained using modified Lanczos technique. The calculations were at $f = 1/2, 1/4$ with system size $N_s = 16$ and at $f = 1/3$ with $N_s = 12$. At a critical repulsion there is a striking discontinuous transition in both $S^*(\pi)$ and n_s ; while $S^*(\pi)$ jumps from its minimum to maximum, there is a significant drop in n_s .

where b_j is the destruction operator for a HCB, $V \geq 0$, $n_j = b_j^\dagger b_j$, and N_s is the total number of sites. We assume periodic boundary conditions and first study numerically (using modified Lanczos algorithm¹³) the quantum phase transition (QPT) in the $t_2 - V$ model. We will characterize the transition through the structure factor and the superfluid density. The structure factor is given by $S(k) = \sum_{l=1}^{N_s} e^{ikl} W(l)$ where $W(l)$ is the two-point correlation function for density fluctuations of HCBs at a distance l apart (when lattice constant is set to unity): $W(l) = \frac{4}{N_s} \sum_{j=1}^{N_s} [\langle n_j n_{j+l} \rangle - \langle n_j \rangle \langle n_{j+l} \rangle]$. The wavevector $k = \frac{2n\pi}{N_s}$ with $n = 1, 2, \dots, N_s$; filling-fraction $f \equiv \langle n_j \rangle = \frac{N_p}{N_s}$ with N_p being the total number of HCBs in the system. For e-rings with $N_s = 2N$ sites, from the definition of the structure factor, for $k = \pi$ we have

$$S(k) = \sum_{l=1}^{2N} (-1)^l W(l). \quad (2)$$

Substituting the expression for the correlation function $W(l)$ and recognizing that $\sum_{l=1}^{2N} e^{i\pi l} = 0$, we get

$$S(k) = \frac{4}{2N} \sum_{j=1}^{2N} \left\langle n_j \sum_{l=1}^{2N} n_{j+l} (-1)^l \right\rangle. \quad (3)$$

In the above equation, on taking $j + l = m$ we get

$$S(k) = \frac{2}{N} \sum_{j=1}^{2N} \left\langle n_j (-1)^j \sum_{m=1}^{2N} n_m (-1)^m \right\rangle. \quad (4)$$

On defining the number operator which gives the total number of HCBs at even (odd) sites as $\hat{N}_e = \sum_{j \text{ even}} n_j$

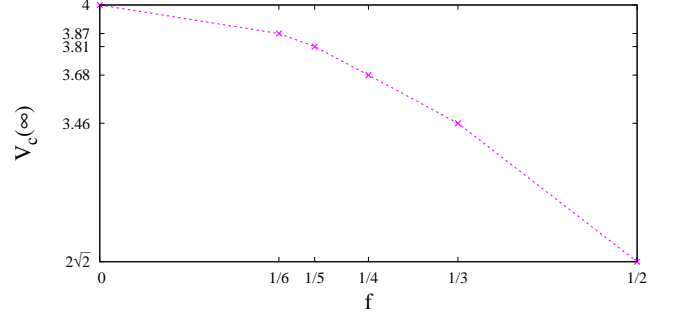


FIG. 2. (Color online) Plot of $V_c(\infty)$ (critical repulsion for an infinite system) obtained from Green's function analysis for half-filled ($f = 1/2$) and two HCB systems ($f \rightarrow 0$) and from finite size scaling at various other fillings f .

($\hat{N}_o = \sum_{j \text{ odd}} n_j$), we obtain

$$S(\pi) = \frac{2\langle (\hat{N}_e - \hat{N}_o)^2 \rangle}{N}. \quad (5)$$

Due to the presence of only next-nearest-neighbor hopping, both \hat{N}_e and \hat{N}_o commute with the $t_2 - V$ Hamiltonian; hence we obtain the following result

$$S(\pi) = \frac{2(N_e - N_o)^2}{N}, \quad (6)$$

where N_e (N_o) are the total number of HCBs at even (odd) sites. Thus the minimum value of $S(\pi) = 0$ corresponds to equal number of particles in both the sublattices whereas the maximum is given by

$$[S(\pi)]_{\text{max}} = \frac{2N_p^2}{N} = \frac{4N_p^2}{N_s}, \quad (7)$$

indicating a single sublattice occupancy. To study the QPT, we rescale the value of $S(\pi)$ as $S^*(\pi) = \frac{S(\pi)}{[S(\pi)]_{\text{max}}}$ with $S^*(\pi)$ representing the order parameter that varies from 0 to 1 during the phase transition.

Next, we will outline our procedure for calculating the superfluid density by threading the chain with an infinitesimal magnetic flux θ . The superfluid fraction is given by^{14,15}

$$n_s = \frac{N^2}{N_p t_{\text{eff}}} \left[\frac{1}{2} \frac{\partial^2 E(\theta)}{\partial \theta^2} \right]_{\theta=0}, \quad (8)$$

where $E(\theta)$ is the total energy when threaded by flux θ and $t_{\text{eff}} = \hbar^2/2m$ is the effective hopping term which for our $t_2 - V$ model is given by $t_{\text{eff}} = 4t_2$.

The total energy for the case $V > V_c$, when threaded by a flux θ , is expressed as

$$E(\theta) = -2t_2 \sum_k \cos[2(k + \theta/N_s)], \quad (9)$$

where $N_s = 2N$. Then, from the above definition of superfluid density n_s , for $V > V_c$, we have

$$n_s = \frac{1}{N_p} \sum_k \cos(2k). \quad (10)$$

Since we consider even values of N_p , the momenta occupied by the HCBs are $k = \frac{(2m+1)\pi}{2N}$ with $-\frac{N_p}{2} \leq m \leq \frac{N_p}{2} - 1$. Summing over these momenta, for the case of single sublattice occupancy (which occurs when $V > V_c$), we have from expression (10)

$$n_s = \frac{1}{N_p} \frac{\sin\left(\frac{\pi N_p}{N}\right)}{\sin\left(\frac{\pi}{N}\right)}. \quad (11)$$

When both the sublattices are equally occupied (i.e., for $V = 0$), in each sublattice of N sites we have $\frac{N_p}{2}$ particles. Thus, the superfluid density in this case takes the form

$$n_s = \frac{2}{N_p} \frac{\sin\left(\frac{\pi N_p}{2N}\right)}{\sin\left(\frac{\pi}{N}\right)}. \quad (12)$$

When e-rings were used, at all fillings f , we found that the order parameter $S^*(\pi)$ jumps from 0 to 1 at a critical value of repulsion V_c indicating that the system transits from equally populated sub-lattices (i.e., Ising symmetry) case to a single sub-lattice occupancy, i.e., a period-doubling CDW state [see Fig. 1]. Concomitantly, as can be seen from Fig. 1, there is a sudden drop in the superfluid fraction n_s at the same critical repulsion. At half-filling, where the superfluid fraction vanishes above a critical repulsion because a single sub-lattice is completely filled, the transition shows that superfluidity and CDW state are mutually exclusive. On the other hand, at all non-half-fillings, we see that the system undergoes a QPT from a superfluid to a supersolid (i.e., a homogeneously coexisting superfluid and CDW) state. In Fig. 1, it is of interest to note that the values of n_s at $V = 0$ and $V > V_c$ are exactly those predicted by Eq. (11) and Eq. (12), respectively.

Next, for e-rings at various fillings, we relate $V_c(2N)$ (critical repulsion at $N_s = 2N$) to $V_c(\infty)$ using finite size scaling analysis (see Appendix A for details) and obtain Fig. 2. At half-filling, from finite size scaling analysis we obtain that $V_c(\infty) \approx 2.83$; in the next section, we show (using Green's function analysis) the exact result $V_c(\infty) = 2\sqrt{2}$. For systems with 2 HCB and $N_s = 4, 6, 8, 10, 12, 14, 16, 18,$ and 20 , we find numerically that $V_c \approx 4.00$; in the next section, we obtain the exact result (using Green's functions) that $V_c(2N) = 4$ for any system size $N_s = 2N \geq 4$.

III. EXACT INSTABILITY CONDITION AT HALF-FILLING IN e-rings

We study the following t_2 - V Hamiltonian in rings with even number of sites ($2N$) by considering two sublattices

C and D and using periodic boundary conditions:

$$H \equiv -t_2 \sum_{i=1}^N (c_i^\dagger c_{i+1} + \text{H.c.}) - t_2 \sum_{i=1}^N (d_i^\dagger d_{i+1} + \text{H.c.}) + V \sum_{i=1}^N d_i^\dagger d_i (c_i^\dagger c_i + c_{i-1}^\dagger c_{i-1}), \quad (13)$$

where c and d denote destruction operators of HCBs in sublattices C and D , respectively.

To understand the discontinuous phase transition at half-filling, (i.e., the transition from equal occupation of both sublattices to occupation of only one sublattice at a critical V_c) we begin by recognizing that when the system is on the verge of completing the phase transition, the system will pass through the state where there is one HCB in one sublattice and one hole in the other sublattice. Hence, we now consider instability for the case of one particle in sublattice C and one hole [with destruction operator denoted by h ($\equiv d^\dagger$)] in sublattice D ; we then rearrange the above equation as

$$H \equiv -t_2 \sum_{i=1}^N (c_i^\dagger c_{i+1} + \text{H.c.}) + t_2 \sum_{i=1}^N (h_i^\dagger h_{i+1} + \text{H.c.}) - V \sum_{i=1}^N (h_i^\dagger h_i - 1)(c_i^\dagger c_i + c_{i-1}^\dagger c_{i-1}). \quad (14)$$

We define the particle-hole Green's function as follows¹⁶:

$$g_n^h \equiv {}_h\langle k, 0 | G(\omega) | k, n \rangle_h, \quad (15)$$

where $G(\omega) \equiv 1/(\omega + i\eta - H)$ and $|k, n\rangle_h$ is the particle-hole state

$$|k, n\rangle_h = \frac{1}{\sqrt{N}} \sum_{j=1}^N e^{ik(j+\frac{\pi}{2})} c_j^\dagger h_{j+n}^\dagger |0\rangle, \quad (16)$$

with k being the total momentum of the particle-hole system and n the separation between the particle and the hole. Using the condition

$$\delta_{0,n} \equiv {}_h\langle k, 0 | G(\omega)(\omega + i\eta - H) | k, n \rangle_h, \quad (17)$$

for $n = 0$, we obtain

$$\begin{aligned} (\omega + i\eta)g_0^h &= 1 + {}_h\langle k, 0 | G(\omega)(H) | k, 0 \rangle_h \\ &= 1 + Vg_0^h - i2t_2 \sin(k/2)g_1^h \\ &\quad + i2t_2 \sin(k/2)g_{-1}^h. \end{aligned} \quad (18)$$

From Eq. (17), for $n = 1$, we get

$$\begin{aligned} (\omega + i\eta)g_1^h &= {}_h\langle k, 0 | G(\omega)(H) | k, 1 \rangle_h \\ &= Vg_1^h - i2t_2 \sin(k/2)g_2^h \\ &\quad + i2t_2 \sin(k/2)g_0^h. \end{aligned} \quad (19)$$

Similarly, for $n \neq 0, 1$, we derive

$$\begin{aligned} (\omega + i\eta)g_n^h &= {}_h\langle k, 0 | G(\omega)(H) | k, n \rangle_h \\ &= 2Vg_n^h - i2t_2 \sin(k/2)g_{n+1}^h \\ &\quad + i2t_2 \sin(k/2)g_{n-1}^h. \end{aligned} \quad (20)$$

As V is increased to the critical repulsion V_c , the HCB in sublattice C vacates its sublattice and enters the sublattice D containing the hole; the energy of the system then becomes 0. Next, we let

$$\frac{\omega + i\eta - 2V}{F_k} \equiv \frac{1}{z} - z, \quad (21)$$

where $F_k \equiv i2t_2 \sin(k/2)$. Then, Eq. (20) takes the simple form

$$\left(\frac{1}{z} - z\right) g_n^h = g_{n-1}^h - g_{n+1}^h, \quad (22)$$

whose solution is of the form

$$g_n^h = \alpha_1^\pm z^n + \frac{\beta_1^\pm}{(-z)^n}, \quad (23)$$

where α_1^+ (α_1^-) and β_1^+ (β_1^-) correspond to $n > 1$ ($n < 0$). The transition occurs at the critical value of V that makes the overall energy 0. Let $V = 2t_2\gamma \sin(k/2)$. The overall energy is less than $-4t_2 + 2V$ (for $V > 0$). It is important to note that, for the groundstate, $k = \pi$ for any $V \leq V_c$. This can be seen by first noting that when $V = 0$, total momentum in the minimum energy state is π ; next, turning on V does not change the total momentum. Then for $k = \pi$, to get overall energy to be 0, we need the inequality $\gamma > 1$. The instability condition corresponds to the case $\omega = 0$ because then the Green's function g_0^h diverges when the energy is zero. It then follows from Eq. (21) that

$$i2\gamma = \frac{1}{z} - z, \quad (24)$$

which implies that

$$z = i(-\gamma + \sqrt{\gamma^2 - 1}), \quad (25)$$

and hence $|z| < 1$ for $\gamma > 1$. Let us first consider the case $n > 1$. From the above Eq. (23), it is clear that, for $n \rightarrow \infty$, g_n^h is finite only for $\beta_1^+ = 0$. Thus for $n > 1$,

$$g_{n+1}^h = z g_n^h, \quad (26)$$

which implies that $g_3^h = z g_2^h$; then, from Eq. (22) it follows that

$$g_2^h = z g_1^h. \quad (27)$$

Next, for the case $n < 0$, we see that g_n^h is finite, for $n \rightarrow -\infty$, only when $\alpha_1^- = 0$. Thus for $n < 0$,

$$g_{n-1}^h = -z g_n^h, \quad (28)$$

which implies that $g_{-2}^h = -z g_{-1}^h$; then from Eq. (22) we obtain

$$g_{-1}^h = -z g_0^h. \quad (29)$$

From Eqs. (18), (19), (27), and (29), we obtain

$$g_0^h = \frac{1}{(\omega + i\eta - V + zF_k) + \frac{F_k^2}{(\omega + i\eta - V + zF_k)}}, \quad (30)$$

and

$$g_1^h = \frac{g_0^h F_k}{(\omega + i\eta - V + zF_k)}, \quad (31)$$

where $\omega = 0$, $V = 2t_2\gamma$, $z = i(-\gamma + \sqrt{\gamma^2 - 1})$, and $F_k = i2t_2$. It then follows that g_0^h diverges when $(V - zF_k)^2 + F_k^2 = 0$, i.e., when $\gamma = \sqrt{2}$. Thus the instability condition is $V_c = 2\sqrt{2}t_2$. (We now see that the total energy at transition is indeed less than $-4t_2 + 2V$). It is important to note [as can be seen from Eq. (31)] that, when g_0^h diverges, g_1^h also diverges; consequently, from Eqs. (26), (28), and (29) we see that all g_n^h diverge (i.e., even when $n > 1$ and $n < 0$).

IV. EXACT INSTABILITY CONDITION FOR TWO HCBs IN e-rings

We now study the non-trivial case of the two-HCB instability for the $t_2 - V$ Hamiltonian [described by Eq. (13)] in e-rings. We consider one HCB in sublattice C and one HCB in sublattice D; the corresponding two-particle Green's function is defined as $g_n \equiv \langle k, 0 | G(\omega) | k, n \rangle$ with $G(\omega)$ being defined as before and the two-particle state $|k, n\rangle$ being expressed as

$$|k, n\rangle = \frac{1}{\sqrt{N}} \sum_{j=1}^N e^{ik(j+\frac{n}{2})} c_j^\dagger d_{j+n}^\dagger |0\rangle, \quad (32)$$

with k representing the total momentum of the two-particle system. Then, the following equations hold for the Green's functions g_n :

$$\begin{aligned} (\omega + i\eta - V)g_0 &= 1 - 2t_2 \cos(k/2)g_1 \\ &\quad - 2t_2 \cos(k/2)g_{-1}, \end{aligned} \quad (33)$$

$$\begin{aligned} (\omega + i\eta - V)g_1 &= -2t_2 \cos(k/2)g_2 \\ &\quad - 2t_2 \cos(k/2)g_0, \end{aligned} \quad (34)$$

and for $n \neq 0, 1$

$$\begin{aligned} (\omega + i\eta)g_n &= -2t_2 \cos(k/2)g_{n+1} \\ &\quad - 2t_2 \cos(k/2)g_{n-1}. \end{aligned} \quad (35)$$

As V increases to the critical V_c , the energy given by Eq. (13) becomes $-4t_2 \cos(\pi/N)$ (i.e., the minimum energy of the two HCBs in the same sublattice); this would correspond to the instability where one HCB quits its sublattice and goes into the sublattice of the other particle. Here, we make the key observation that $k = 0$ for the groundstate at any V . To understand this, we first note for $V = 0$, the total momentum is zero in the minimum energy state; next, we recognize that turning on V does not change the total momentum. Now, to obtain the instability, we take

$$\begin{aligned} \frac{\omega}{(-2t_2)} &= \frac{4t_2 \cos(\pi/N)}{2t_2} = 2 \cos(\pi/N) \\ &= e^{i\pi/N} + e^{-i\pi/N} \\ &= z + \frac{1}{z}. \end{aligned} \quad (36)$$

We set $z = e^{i\pi/N}$ and also take $V/(2t_2) = 2\gamma$. Then, Eqs. (33), (34), and (35) become

$$[(z + 1/z) + 2\gamma]g_0 = -1/(2t_2) + g_1 + g_{-1}, \quad (37)$$

$$[(z + 1/z) + 2\gamma]g_1 = g_2 + g_0, \quad (38)$$

and for $n \neq 0, 1$

$$[(z + 1/z)]g_n = g_{n+1} + g_{n-1}. \quad (39)$$

Without loss of generality, we assume

$$g_1 = \alpha_2 z + \beta_2/z, \quad (40)$$

and

$$g_2 = \alpha_2 z^2 + \beta_2/z^2. \quad (41)$$

Then using Eqs. (39), (40), and (41), we obtain for $n = 3, 4, \dots, N$ the expression

$$g_n = \alpha_2 z^n + \beta_2/z^n. \quad (42)$$

It is important to recognize that $|z| = 1$; hence, the Green's functions do not decay with HCB separation n . Next, we note that at $k = 0$, $|k, -n\rangle = |k, N - n\rangle$; consequently, we see that $g_N = g_0$ and $g_{N-1} = g_{-1}$. Then, using Eq. (42) and the relation $z = e^{i\pi/N}$, we get

$$\begin{aligned} g_{-1} = g_{N-1} &= \alpha_2 z^{N-1} + \beta_2/z^{N-1} \\ &= -(\alpha_2/z + \beta_2 z), \end{aligned} \quad (43)$$

and

$$\begin{aligned} g_0 = g_N &= \alpha_2 z^N + \beta_2/z^N \\ &= -(\alpha_2 + \beta_2). \end{aligned} \quad (44)$$

We are now ready to solve for the Green's functions g_n using Eqs. (37), (38), (40), (41), (43), and (44). We get the following equations:

$$\alpha_2[z + \gamma] + \beta_2[1/z + \gamma] = 1/(4t_2), \quad (45)$$

and

$$\alpha_2[1 + \gamma z] + \beta_2[1 + \gamma/z] = 0. \quad (46)$$

It then follows from the above two equations that

$$\alpha_2 = \frac{z + \gamma}{4t_2(z^2 + \gamma^2 - 1 - \gamma^2 z^2)}, \quad (47)$$

which diverges when $\gamma = \pm 1$. We get $\gamma = 1$ for repulsive V . Furthermore,

$$\beta_2 = -\alpha_2 \frac{1 + \gamma z}{1 + \gamma/z}, \quad (48)$$

which for $\gamma = 1$ yields $\beta_2 = -\alpha_2 z$. Thus we see that $g_0 = -(\alpha_2 + \beta_2) = -\alpha_2(1 - z)$ diverges for $\gamma = 1$ or $V_c = 4t_2$. We also find that for $0 \neq n \leq N$

$$g_n = \alpha_2 z^n + \beta_2/z^n = \alpha_2 \left(e^{i\pi n/N} - e^{-i\pi(n-1)/N} \right), \quad (49)$$

also diverges since $2n - 1 \neq 2N$. *The instability condition $V_c = 4t_2$ is independent of N and hence is valid for large N as well!* Another interesting observation based on $\beta_2 = -\alpha_2 z$ is that

$$\begin{aligned} g_{-k} = g_{N-k} &= -\alpha_2/z^k - \beta_2 z^k \\ &= \beta_2/z^{k+1} + \alpha_2 z^{k+1} \\ &= g_{k+1}. \end{aligned} \quad (50)$$

V. NUMERICAL STUDY OF THE $t_2 - V$ MODEL FOR o-rings

We calculate the structure factor at large repulsion so that the CDW would be better defined (with larger values for the structure factor) even for finite number of sites. Since the allowed momenta for HCBs in o-rings (with $2N + 1$ sites) are $k = \frac{2n\pi}{2N+1}$ with $n=1,2,\dots,2N+1$; the structure factor $S(k)$ will have peaks at $k = Q \equiv \pi \pm \frac{\pi}{2N+1}$; in fact π is not an allowed value for the momentum k !. For $k = Q = \pi + \frac{\pi}{2N+1}$ we have

$$\begin{aligned} S(Q) &= \sum_{l=1}^{2N+1} e^{i(\pi + \frac{\pi}{2N+1})l} W(l) \\ &= \sum_{l=1}^{2N+1} (-1)^l e^{i(\frac{\pi}{2N+1})l} W(l). \end{aligned} \quad (51)$$

Substituting the expression for $W(l)$ and ignoring the term $\langle n_j \rangle \langle n_{j+l} \rangle = \langle n_j \rangle^2$ in $W(l)$ (because $\sum_{l=1}^{2N+1} e^{i(\pi + \frac{\pi}{2N+1})l} = 0$) we get

$$S(Q) = \frac{4}{2N+1} \sum_{j=1}^{2N+1} \left\langle n_j \sum_{l=1}^{2N+1} n_{j+l} (-1)^l e^{i(\frac{\pi}{2N+1})l} \right\rangle. \quad (52)$$

In the above equation, setting $j + l = m$ yields

$$\begin{aligned} S(Q) &= \frac{4}{2N+1} \sum_{j=1}^{2N+1} \left\langle n_j (-1)^j e^{-i(\frac{\pi}{2N+1})j} \right. \\ &\quad \times \left. \sum_{m=1}^{2N+1} n_m (-1)^m e^{i(\frac{\pi}{2N+1})m} \right\rangle. \end{aligned} \quad (53)$$

At large repulsion all the particles in o-rings will be confined to N alternate sites similar to the case of e-rings (with $2N$ sites). First, we consider the filling

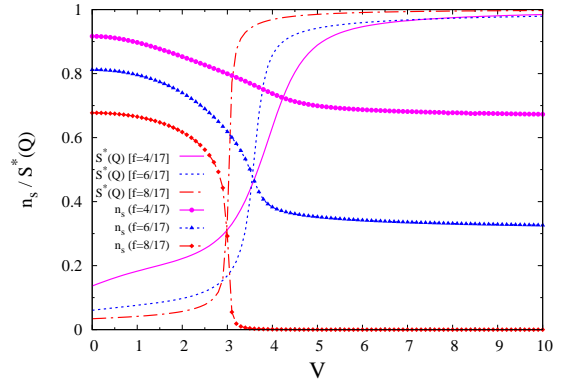


FIG. 3. (Color online) Plots of rescaled structure factor $S^*(Q) \equiv S(Q)/[S(Q)]_{\max}$ (with $Q = \pi \pm \frac{\pi}{2N+1}$) and superfluid fraction n_s at various fillings f obtained using modified Lanczos method. At a critical repulsion there is a sharp rise in $S^*(Q)$ with a concomitant significant drop in n_s .

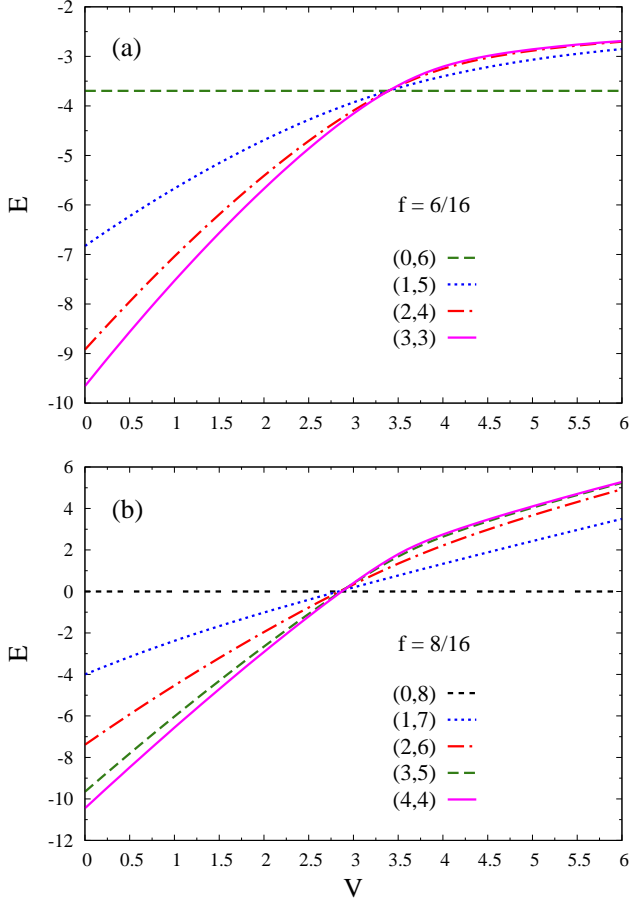


FIG. 4. (Color online) Plots of energy E versus repulsion V for (a) the lowest energy states with $(m,6-m)$ particles in e-ring with $N_s = 16$ and $N_p = 6$ (non-half filled case); and (b) the lowest energy states with $(m,8-m)$ particles in e-ring with $N_s = 16$ and $N_p = 8$ (half-filled case).

$f = N/(2N + 1)$ (i.e., $N_p = N$). Consequently, the maximum value of the structure factor is given by

$$\begin{aligned}
 [S(Q)]_{\max} &= \frac{4}{2N+1} \left[\frac{N_p}{N} (-1) e^{-i\frac{\pi}{2N+1}} + \frac{N_p}{N} (-1)^3 e^{-i\frac{3\pi}{2N+1}} \right. \\
 &\quad \left. + \dots + \frac{N_p}{N} (-1)^{2N-1} e^{-i\frac{(2N-1)\pi}{2N+1}} \right] [\text{H.c.}] \\
 &= \frac{2}{2N+1} \left(\frac{N_p}{N} \right)^2 \left(\frac{1}{1 - \cos\left(\frac{\pi}{2N+1}\right)} \right), \quad (54)
 \end{aligned}$$

with $N_p = N$ for $f = N/(2N + 1)$. For the $N_p = N$ case, the above expression for $[S(Q)]_{\max}$ is exact at all values of N (see Table I).

In the thermodynamic limit ($2N + 1 \rightarrow \infty$), the above expression for $[S(Q)]_{\max}$ diverges as

$$[S(Q)]_{\max} = \frac{4}{\pi^2} \left(\frac{4N_p^2}{2N+1} \right) = \frac{4}{\pi^2} \left(\frac{4N_p^2}{N_s} \right). \quad (55)$$

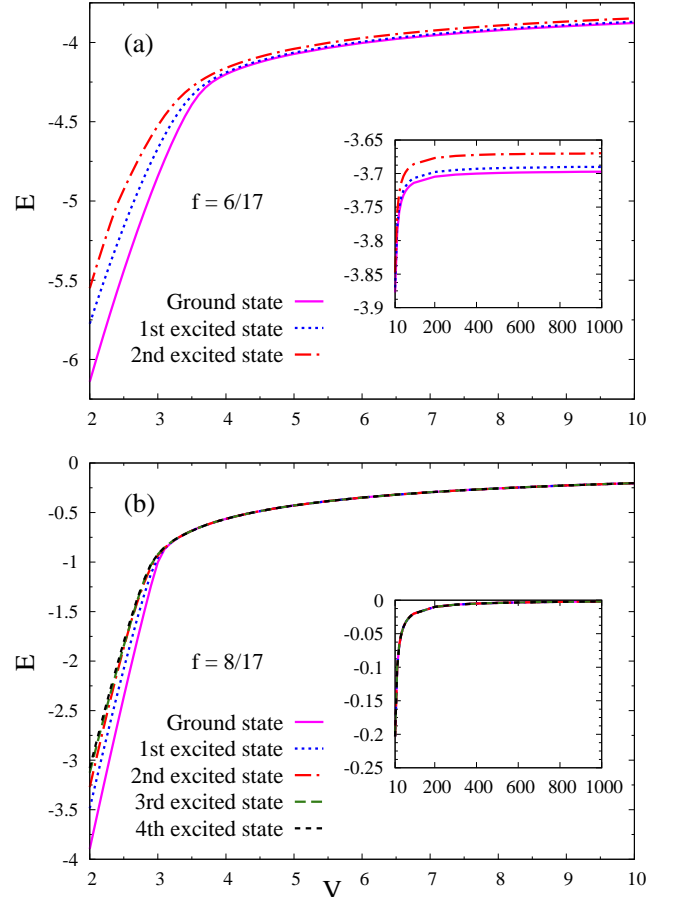


FIG. 5. (Color online) Plots of energy E versus repulsion V for (a) the three lowest energy states in o-ring with $N_s = 17$ and $N_p = 6$; and (b) the five lowest energy states in o-ring with $N_s = 17$ and $N_p = 8$.

We rescale $S(Q)$ as

$$S^*(Q) = \frac{S(Q)}{[S(Q)]_{\max}}. \quad (56)$$

For $N_p < N$, all the N sites considered for particle occupation would be connected through hopping so that the total energy is minimized, i.e., the potential energy is zero and the kinetic energy is minimized. Next, we

N_p/N_s	Analytical value of $[S(Q)]_{\max}$	Numerical value of $[S(Q)]_{\max}$		
		$V=50$	$V=100$	$V=500$
$\frac{4}{9}$	3.6848	3.6836	3.6845	3.6848
$\frac{6}{13}$	5.2944	5.2935	5.2942	5.2944
$\frac{8}{17}$	6.9095	6.90878	6.9093	6.9095
$\frac{10}{21}$	8.5269	8.5263	8.5267	8.5269

TABLE I. At filling fraction $f = \frac{N}{(2N+1)}$, the numerical value of $[S(Q)]_{\max}$ calculated at large V agrees quite well with the analytic value obtained from Eq. (54).

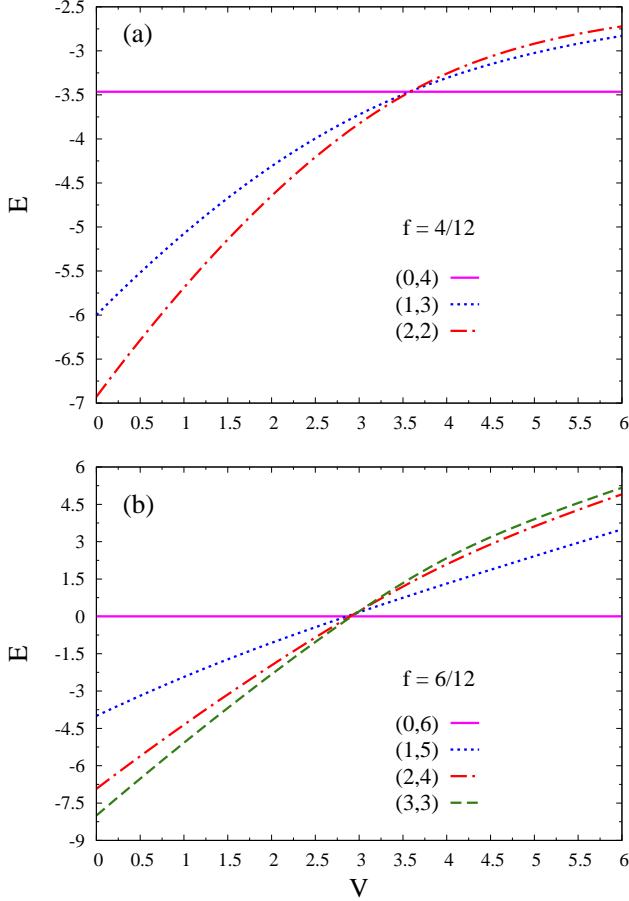


FIG. 6. (Color online) Plots of energy E versus repulsion V for (a) the lowest energy states with $(m, 4-m)$ particles in e-ring with $N_s = 12$ and $N_p = 4$ (non-half filled case); and (b) the lowest energy states with $(m, 6-m)$ particles in e-ring with $N_s = 12$ and $N_p = 6$ (half-filled case)

assume that the N_p particles are uniformly distributed among these N alternate sites; such an assumption is valid for large values of N as the end effects (i.e., at the boundary of the N alternate sites) is negligible. Then, for $N_p < N$, the expression (54) is approximate at finite N (see Table II) and exact for $N \rightarrow \infty$. Furthermore, the expression for the peak value of the structure factor for e-rings [given by Eq. (7)] differs from that for o-rings [given by Eq. (55)] due to the phase factor $e^{-i(\frac{\pi}{2N+1})m}$ in Eq. (54); interestingly the difference is not negligible in the thermodynamic limit (i.e., $2N + 1 \rightarrow \infty$).

Next, we will outline our procedure for calculating the superfluid density for o-rings at $V = 0$. From the definition of superfluid density n_s it is obvious that, to calculate n_s , all we need is to calculate the total energy $E(\theta)$ which is independent of whether the particles are fermions or hard-core-bosons. So, if we recast our system in terms of fermions, the boundary condition turns out to be

$$e^{ik(2N+1)2} = -1 = e^{i(2m+1)\pi}, \quad (57)$$

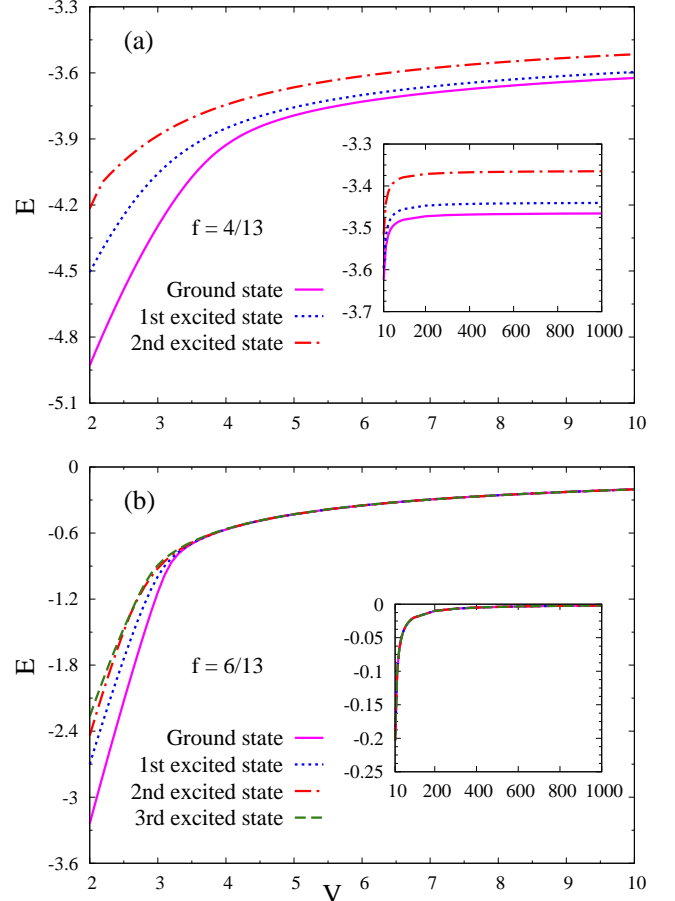


FIG. 7. (Color online) Plots of energy E versus repulsion V for (a) the three lowest energy states in o-ring with $N_s = 13$ and $N_p = 4$; and (b) the four lowest energy states in o-ring with $N_s = 13$ and $N_p = 6$.

where m is an integer. The above equation implies that

$$k = \frac{(2m+1)\pi}{2(2N+1)} \quad \text{with} \quad -\frac{N_p}{2} \leq m \leq \frac{N_p}{2} - 1.$$

So, for $V = 0$, we obtain the superfluid density for o-rings

$$\begin{aligned} n_s &= \frac{1}{N_p} \sum_{k=-\frac{\pi(N_p-1)}{2(2N+1)}}^{\frac{\pi(N_p-1)}{2(2N+1)}} \frac{(e^{2ik} + e^{-2ik})}{2} \\ &= \frac{1}{N_p} \frac{\sin\left(\frac{\pi N_p}{2N+1}\right)}{\sin\left(\frac{\pi}{2N+1}\right)}. \end{aligned} \quad (58)$$

When o-rings are considered, we find that at all fillings f the structure factor $S^*(Q)$ shows a sharp increase at a critical value of repulsion V_c ; concomitantly, there is a sharp drop in the superfluid fraction n_s at the same critical repulsion V_c (see Fig. 3). For finite systems, at large V , n_s values are the same for e-rings and o-rings at fillings $f = N_p/(2N)$ and $f = N_p/(2N+1)$, respectively.

N_p/N_s	Analytical value of $[S(Q)]_{\max}$	Numerical value of $[S(Q)]_{\max}$		
		V=50	V=100	V=500
$\frac{6}{15}$	4.4828	4.4574	4.4618	4.4650
$\frac{6}{17}$	3.8866	3.8634	3.8691	3.8734
$\frac{6}{19}$	3.4302	3.4124	3.4183	3.4228
$\frac{6}{21}$	3.0697	3.0566	3.0623	3.0668
$\frac{8}{19}$	6.0982	6.0702	6.0740	6.0766
$\frac{8}{21}$	5.4572	5.4264	5.4316	5.4355

TABLE II. At filling fraction $f = \frac{N_p}{(2N+1)}$ with $N_p < N$, the analytical value of $[S(Q)]_{\max}$ [obtained from Eq. (54)] approximates reasonably well the numerical value at large V .

In the thermodynamic limit, we expect a first order CDW transition, with the structure factor jumping at a critical V similar to the case in Fig. 1 for e-rings (although, magnitude-wise, $[S(Q)]_{\max}$ for o-rings is $\frac{4}{\pi^2}$ of the structure factor $[S(\pi)]_{\max}$ for e-rings); simultaneously, at the same critical V we expect a sudden drop in n_s similar to Fig. 1. At filling $N/(2N+1)$ the superfluid fraction decreases to zero, whereas at all lower fillings [i.e., $N_p/(2N+1)$ with $N_p < N$] it transits to a nonzero value. Thus, at filling $N/(2N+1)$, superfluidity and CDW state are mutually exclusive; whereas, at all fillings $N_p/(2N+1)$ with $N_p < N$ the system undergoes a transition from a superfluid to a supersolid.

VI. COMPARISON BETWEEN e-rings AND o-rings

In our $t_2 - V$ model, e-rings have two similar homogeneous Fermi seas whose occupational symmetry is broken at a critical repulsion to populate only one non-interacting Fermi sea thereby producing a supersolid

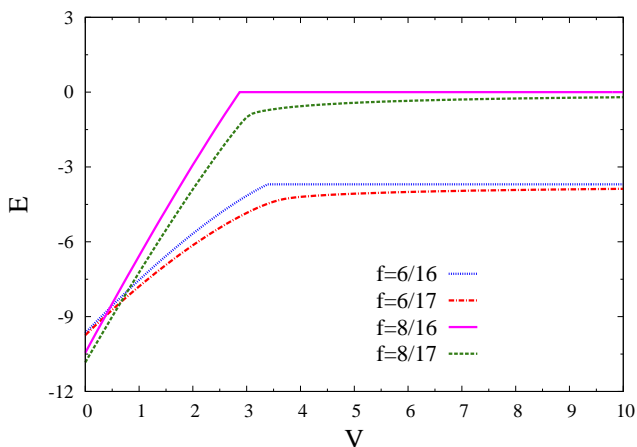


FIG. 8. (Color online) Plots of energy E versus repulsion V for groundstate at various fillings $f = N_p/N_s$.

(CDW) at non-half (half) filling. The situation for o-rings, corresponds to a single band breaking up into two bands with a midgap state.

From the energy versus V plots for e-rings (in Figs. 4 and 6), we note that for different finite systems with even number of sites (both for half and non-half fillings) the various lowest energy levels [with particle distribution $(m, N_p - m)$] cross at a critical V ; from this and our Green's function analysis above, we conclude that in the thermodynamic limit the system will undergo a first order phase transition at all fillings. On the other hand, for o-rings, since the system has all sites connected through NNN hopping (much like a Moebius strip), there do not exist two sub-lattices. Consequently, when we plotted the lowest few energy states for a finite odd number of sites, there is no energy level crossing at any repulsion V for various fillings considered; the curves monotonically increase with repulsion [see Fig. 5 and 7].

For fillings $f = N/(2N+1)$, we observe that beyond some critical repulsion (close to the value where levels cross in half-filled e-ring with $N_s = 2N$) all the energy levels merge and become degenerate. For filling fractions $f = N_p/(2N+1)$ (with $N_p < N$), the energy levels come close to each other at a critical V that is close to the point where levels cross for e-rings with $f = N_p/(2N)$; a little beyond this critical V , the gap between any two energy levels becomes constant and remains the same even at large V . The insets in Figs. 5(a), 5(b), 7(a), and 7(b), show that at large V the graphs remain more or less unchanged. Thus, for finite systems with odd number of sites, the energy levels never cross each other. Still, we expect that in the thermodynamic limit the ground state of an o-ring will be similar to that of an e-ring and thus will have a kink at the same critical repulsion V_c . As a result, in the thermodynamic limit, we expect both the systems to have a similar kind of phase transition. Another important point to note, as $V \rightarrow \infty$, is that the ground state energy of o-rings at $f = N_p/(2N+1)$ approaches (from below) the ground state energy of e-rings at $f = N_p/(2N)$ [see Fig. 8]. Consequently, the superfluid fraction takes the same value for both the cases in the limit of large V (see Table III).

However, in the macroscopic limit, the energy spectrum is not expected to be the same for the two cases; for instance, there is a mid-gap state for the odd case which is not there for the even case. The key difference between the rings with even and odd number of sites seems to be the difference in the peak value of the structure factor at large V (above critical V) for finite (infinite) systems. In the thermodynamic limit we expect the structure factors for both o-rings and e-rings to diverge, but their ratio will still be $\frac{4}{\pi^2}$.

For finite e-rings, it is also important to point out our finding that the energy levels cross each other at approximately the same critical repulsion. From the plots of E versus V at a fixed filling fraction f and different system sizes N_s [such as in Figs. 4(b) and 6(b)], we observe that the crossing points get closer as the system size in-

N_p/N_s	Superfluid fraction n_s		
	$V=50$	$V=100$	$V=500$
$\frac{6}{16}$	0.3080	0.3080	0.3080
$\frac{6}{17}$	0.3114	0.3096	0.3080
$\frac{6}{18}$	0.4220	0.4220	0.4220
$\frac{6}{19}$	0.4257	0.4240	0.4226
$\frac{4}{16}$	0.6533	0.6533	0.6533
$\frac{4}{17}$	0.6574	0.6554	0.6537
$\frac{4}{20}$	0.7694	0.7694	0.7694
$\frac{4}{21}$	0.7721	0.7708	0.7698

TABLE III. The superfluid fraction n_s for o-ring at filling $f = N_p/(2N + 1)$ approaches the value of the superfluid fraction for e-ring with $f = N_p/(2N)$ in the large- V limit.

creases. From this we can expect that, in the thermodynamic limit, all the energy levels will cross at the same transition point.

VII. BOSE-EINSTEIN CONDENSATION

Here, we do not calculate the Bose-Einstein condensate occupation number n_0 because, for a system of HCBs in a one-dimensional tight-binding lattice, it varies as $C(f)\sqrt{N}$ in the thermodynamic limit with the coefficient $C(f)$ depending on filling f ^{17,18}; consequently, the condensate fraction $n_0/N_p \propto 1/\sqrt{N} \rightarrow 0$. Next, in the presence of repulsion (as argued in Ref. 19), we expect the BEC occupation number n_0 to again scale as \sqrt{N} ; however, the coefficient of \sqrt{N} will be smaller due to the restriction on hopping imposed by repulsion.

VIII. CONNECTION TO OTHER MODELS

Our $t_2 - V$ model can be mapped onto an extremely anisotropic Heisenberg model (with next-nearest-neighbor XY interaction and nearest-neighbor Ising interaction) by identifying $S^+ = b^\dagger$, $S^- = b$, and $S^z = n - \frac{1}{2}$. The resulting spin Hamiltonian is of the form

$$-t_2 \sum_{i=1}^{N_s} (S_{i-1}^+ S_{i+1}^- + \text{H.c.}) + V \sum_{i=1}^{N_s} S_i^z S_{i+1}^z. \quad (59)$$

While Heisenberg model was amenable to solution through the Bethe ansatz, the addition of next-nearest-neighbor interaction (similar to the case of Majumdar-Ghosh model²⁰) requires an alternate route for its solution. Our spin model lends itself to exact instability solutions (by the Green's function method) in the two limiting cases of two-magnons and antiferromagnetic ground state. The energies at various fillings N_p/N_s for the $t_2 - V$ model correspond to various normalized magnetizations

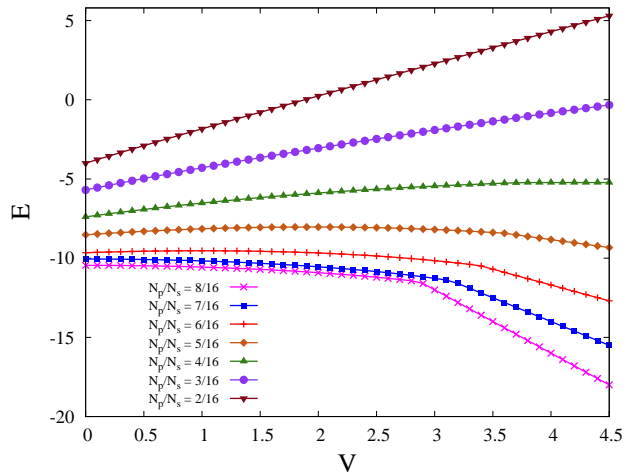


FIG. 9. (Color online) Plots of the lowest energy E (obtained using modified Lanczos in a system with $N_s = 16$ sites) for the extremely anisotropic NNN Heisenberg model at various normalized magnetizations $(N_s - 2N_p)/N_s$ corresponding to fillings $f = N_p/N_s$ for the $t_2 - V$ model.

$(N_s - 2N_p)/N_s$ for the spin model. From a plot of the lowest energies at various magnetizations of the spin model, as depicted in Fig. 9, we see that the energy increases as the normalized magnetization increases with the ground state corresponding to zero magnetization. From the fact that the critical repulsion is always $V_c \leq 4$, it should be clear that the energy at all fillings and system sizes for $V_c > 4$ is obtained from a tight-binding model with N_p particles in one sub-lattice only. Thus at $V_c > 4$, the energy will certainly increase with the normalized magnetization.

Next, in spite of the fact that the hopping terms are different, we note the semblance between our $t_2 - V$ model and the well-known Su-Schrieffer-Heeger (SSH) model²¹. We make the connection that a singlet (formed by two spins on adjacent sites) can be regarded as a HCB located at the center of the singlet¹⁹. Thus a system of HCBs in one sublattice is transformed to a system of singlets with centers located in one sublattice only. At half-filling, for even number of sites, the ground state of the $t_2 - V$ model at V larger than the critical repulsion can be mapped onto a valence-bond ground state of the Su-Schrieffer-Heeger (SSH) model²¹. For an odd number of sites, at filling $N/(2N + 1)$, we can map the ground state at large V with two holes on adjacent sites (i.e., a kink) in the $t_2 - V$ model on to the ground state, with a kink or topological defect (with two single bonds on adjacent sites), in the SSH model. For even number of sites as well, the kinks obtained by doping the valence bond state in the SSH model have a counterpart in our $t_2 - V$ model.

IX. DISCUSSION

Our $t_2 - V$ model is the limiting case of the one-dimensional CBM (cooperative breathing mode) model (i.e., $t_1 - t_2 - V$ model), which depicts a simpler one-band case that is expected to be useful in understanding the CBM physics in real systems such as the bismuthates, the cuprates, and the manganites¹². An important purpose of studying the $t_2 - V$ model is the fact that exact solutions can be obtained analytically for two limiting cases of this model. Till now we do not know how to solve the more complex $t_1 - t_2 - V$ model analytically. We hope that in future our way of solving the two limiting cases of the $t_2 - V$ model analytically (using Green's function technique) will lead to useful approaches to handle more complex problems such as the $t_1 - t_2 - V$ model.

In Ref. 12, $t_2 - V$ model was studied for spinless fermions in e-rings; structure factor $S(\pi)$ and ground state energy were obtained for some filling fractions to show that the system undergoes a discontinuous transition from a Luttinger liquid to a conducting commensurate CDW state away from half filling while at half filling one obtains a Mott insulator. In the present paper, we recast the $t_2 - V$ model in terms of HCBs. Here, along with the structure factor and the ground state energy, we additionally calculate the superfluid fraction. In e-rings, we show that the system undergoes a striking discontinuous transition from a superfluid to either a CDW insulator (at half filling) or a supersolid (at non-half fillings).

In the previous paper¹², only systems with even number of sites was considered, whereas here we also study systems with odd number of sites; we show that supersolidity is realized in o-rings at large repulsion and fillings $N_p/(2N+1)$ with $N_p < N$. When o-rings are considered, at all fillings $N_p/(2N+1)$ with $N_p < N$, the structure factor shows a sharp increase at a critical value of repulsion; simultaneously, there is a sharp drop (to a non-zero value) in the superfluid fraction at the same critical repulsion (see Fig. 3). At $V = 0$, we derived an expression for the superfluid fraction [see Eq. (58)] which matches with the numerical result in Fig. 3. The superfluid fraction, in the limit $V \rightarrow \infty$, for o-rings [at fillings $N_p/(2N+1)$] approaches the value of the superfluid fraction, when $V > V_c$, for e-rings [at fillings $N_p/2N$] – a fact supported by numerical results (see Table III). From the expression for the superfluid fraction in e-rings when $V > V_c$ [see Eq. (11)], it is clear that, for all fillings $N_p/(2N+1)$ with $N_p < N$, we will have non-zero superfluid fraction in o-rings even in the thermodynamic limit. On the other hand, we have also shown that the structure factor $[S(Q)]_{\max}$ calculated analytically for large V agrees quite well with that calculated numerically for sufficiently large systems (see Table II). It is also shown that in the thermodynamic limit, at large V , the structure factor for o-rings appears to be $4/\pi^2$ times the structure factor for e-rings [see Eq. (55)]; as a result we expect the structure factor for o-rings to diverge as $N \rightarrow \infty$. Hence, we can conclude that in the thermodynamic limit, at all

fillings $N_p/(2N+1)$ with $N_p < N$, the system for o-rings exhibits supersolidity (at large V).

As regards relevant work, in Ref. 22 the authors consider nearest-neighbor hopping (and repulsion) and unfrustrated next-nearest-neighbor hopping (and repulsion) that can be realized in a zigzag ladder with two legs. As pointed out in this paper, nearest-neighbor hopping and next-nearest-neighbor hopping can be tuned independently. Thus this work also shows that our $t_2 - V$ model is physically realizable.

Also of relevance is the work by Struck et al.²³ where various values (including sign change) of nearest-neighbor coupling J and next-nearest-neighbor coupling J' can be achieved for hard-core-boson systems. Thus, we feel that our $t_2 - V$ model can be simulated experimentally by introducing repulsions and next-nearest-neighbor coupling J' .

Recently, Mishra et al.^{24,25} studied a one-dimensional system of HCBs, with nearest-neighbor hopping and interaction and next-nearest-neighbor hopping, described by the Hamiltonian

$$H = -t_1 \sum_i (b_i^\dagger b_{i+1} + \text{H.c.}) - t_2 \sum_i (b_i^\dagger b_{i+2} + \text{H.c.}) + \sum_i V (n_i - \frac{1}{2}) (n_{i+1} - \frac{1}{2}). \quad (60)$$

While Pankaj and Yarlagadda¹² considered unfrustrated next-nearest-neighbor hopping, Misra et al.^{24,25} focussed on frustrated hopping. In Ref. 24, at half filling the authors set $t_1 = 1$ and varied t_2 from 0 to $-t_1$ to obtain the total phase diagram containing superfluid, CDW, and bond-ordered phases. At incommensurate densities (non-half fillings) and with $t_2 = -t_1$, the authors of Ref. 25 found a supersolid phase. In Refs. 24 and 25, the competition between two different hopping processes (i.e., hoppings from one site to nearest-neighbor site and to next-nearest-neighbor site with different signs of the hopping terms) gives rise to kinetic frustration in the system. On the other hand, our $t_2 - V$ model depicts the strong EPI limit; as a result there is only one kind of hopping process. Consequently, there is no frustration in our $t_2 - V$ system.

X. CONCLUSIONS

We investigated a model which captures the essential dominant-transport feature of cooperative strong EPI in all dimensions (and in even non-cubic geometries). Our study shows that, compared to the non-cooperative situation, cooperative EPI produces strikingly different physics such as a dramatic superfluid to a supersolid transition with the order parameter jumping to its maximum value. Understanding one-dimensional strong EPI systems, besides being helpful in designing oxide rings, will be of relevance to predicting and controlling the variation of system properties in the direction normal to the interface in oxide heterostructures; needless to say, ox-

ide rings and oxide heterostructures offer extraordinary scientific and technological opportunities²⁶.

XI. ACKNOWLEDGMENTS

S.Y. acknowledges vital discussions with M. Berciu, R. Pankaj, Diptiman Sen, P. B. Littlewood, and G. Baskaran. S.Y. also thanks KITP for hospitality. This work is dedicated to the interactions with and memory of Gabriele F. Giuliani.

Appendix A: Finite size scaling analysis for HCBs in $t_2 - V$ model for e-rings

In this section, we will outline our approach to carrying out finite size scaling analysis for a system with even number of sites. Let us first consider a non-interacting system (with $2N$ sites and N_p particles) described by a tight-binding Hamiltonian. For even number of particles, the ground state has particles occupying momenta $\frac{(2m+1)\pi}{2N}$ with $-N_p/2 \leq m \leq N_p/2 - 1$; whereas for odd number of particles the ground state is represented by particle momenta $\frac{(2m)\pi}{2N}$ with $-(N_p - 1)/2 \leq m \leq (N_p - 1)/2$. Thus the ground state wavefunction (due to the occupied momenta) is an even function of $1/2N$. Now, for the case corresponding to after the phase transition where all the particles are in the same sublattice C, the energy of the ground state $|\phi_0\rangle$ is given by

$$E_I = \sum_{i=1}^N \langle \phi_0 | -t_2(c_i^\dagger c_{i+1} + \text{H.c.}) | \phi_0 \rangle, \quad (\text{A1})$$

where c is the destruction operator for a HCB in sublattice C. Upon taking into account discrete translational symmetry, we get

$$\frac{E_I}{N} = \langle \phi_0 | -t_2(c_i^\dagger c_{i+1} + \text{H.c.}) | \phi_0 \rangle. \quad (\text{A2})$$

Since $|\phi_0\rangle$ is even in $1/2N$, we note that $\frac{E_I}{N}$ is also even in $1/2N$.

Next, consider the interacting system characterized by the following $t_2 - V$ Hamiltonian in rings with even num-

ber of sites ($2N$) and with periodic boundary conditions:

$$H \equiv -t_2 \sum_{i=1}^N (c_i^\dagger c_{i+1} + \text{H.c.}) - t_2 \sum_{i=1}^N (d_i^\dagger d_{i+1} + \text{H.c.}) + V \sum_{i=1}^N d_i^\dagger d_i (c_i^\dagger c_i + c_{i-1}^\dagger c_{i-1}), \quad (\text{A3})$$

where c (d) is the destruction operator for HCB in sublattice C (D) and $V \geq 0$. Upon invoking reflection symmetry, we note that the ground state will be invariant when the sign of momenta is reversed; equivalently the ground state $|\psi_0\rangle$ is an even function of $1/2N$. The ground state energy, before the phase transition, is given by

$$E_{II} = \sum_{i=1}^N \langle \psi_0 | -t_2[(c_i^\dagger c_{i+1} + \text{H.c.}) + (d_i^\dagger d_{i+1} + \text{H.c.})] | \psi_0 \rangle + \sum_{i=1}^N \langle \psi_0 | V d_i^\dagger d_i (c_i^\dagger c_i + c_{i-1}^\dagger c_{i-1}) | \psi_0 \rangle. \quad (\text{A4})$$

Upon recognizing discrete translational invariance, we see that

$$\frac{E_{II}}{N} = \langle \psi_0 | -t_2[(c_i^\dagger c_{i+1} + \text{H.c.}) + (d_i^\dagger d_{i+1} + \text{H.c.})] | \psi_0 \rangle + \langle \psi_0 | V d_i^\dagger d_i (c_i^\dagger c_i + c_{i-1}^\dagger c_{i-1}) | \psi_0 \rangle. \quad (\text{A5})$$

Since, $|\psi_0\rangle$ is even in $1/2N$, it follows that $\frac{E_{II}}{N}$ is also even in $1/2N$.

Now, at the transition point (corresponding to a critical interaction V_c), $\frac{E_{II}}{N} - \frac{E_I}{N} = 0$; this implies that

$$V_c = \frac{\langle \psi_0 | t_2[(c_i^\dagger c_{i+1} + \text{H.c.}) + (d_i^\dagger d_{i+1} + \text{H.c.})] | \psi_0 \rangle}{\langle \psi_0 | d_i^\dagger d_i (c_i^\dagger c_i + c_{i-1}^\dagger c_{i-1}) | \psi_0 \rangle} - \frac{\langle \phi_0 | t_2(c_i^\dagger c_{i+1} + \text{H.c.}) | \phi_0 \rangle}{\langle \phi_0 | d_i^\dagger d_i (c_i^\dagger c_i + c_{i-1}^\dagger c_{i-1}) | \phi_0 \rangle}. \quad (\text{A6})$$

In the above equation, because both numerator and denominator of all the terms on the right-hand side are even in $1/2N$, it follows that V_c is also even in $1/2N$. Thus, for e-rings at various fillings, we relate $V_c(2N)$ (critical repulsion at $N_s = 2N$) to $V_c(\infty)$ as follows:

$$V_c(2N) - V_c(\infty) = \frac{A}{N^2} + \frac{B}{N^4} + \dots, \quad (\text{A7})$$

where A, B, \dots are constants.

It is also important to note that we used general arguments to show that the ground state energy $\frac{E_{II}}{N}$ is even in $1/2N$; these arguments can be extended to show that the ground state energies of other interacting systems such as the $t - V$ model are also even functions of $1/2N$. The fact that the ground state energy of the $t - V$ model is an even function of $1/2N$ has been used in Ref. 13.

-
- ¹ H. Y. Hwang, Y. Iwasa, M. Kawasaki, B. Keimer, N. Nagaosa and Y. Tokura, *Nature Materials* **11**, 103 (2012).
 - ² For a review, see T. Hotta, *Rep. Prog. Phys.* **69**, 2061 (2006).
 - ³ S. H. Blanton, R. T. Collins, K. H. Kelleher, L. D. Rotter, Z. Schlesinger, D. G. Hinks, and Y. Zheng *Phys. Rev. B* **47**, 996 (1993).
 - ⁴ A. Rusydi, W. Ku, B. Schulz, R. Rauer, I. Mahns, D. Qi, X. Gao, A. T. S. Wee, P. Abbamonte, H. Eisaki, Y. Fujimaki, S. Uchida, and M. Rübhausen, *Phys. Rev. Lett.* **105**, 026402 (2010); P. Abbamonte, G. Blumberg, A. Rusydi, A. Gozar, P. G. Evans, T. Siegrist, L. Venema, H. Eisaki, E. D. Isaacs, and G. A. Sawatzky, *Nature (London)* **431**, 1078 (2004).
 - ⁵ A. Lanzara, P. V. Bogdanov, X. J. Zhou, S. A. Kellar, D. L. Feng, E. D. Lu, T. Yoshida, H. Eisaki, A. Fujimori, K. Kishio, J.-I. Shimoyama, T. Noda, S. Uchida, Z. Hussain, and Z. X. Shen, *Nature (London)* **412**, 510 (2001).
 - ⁶ G.-H. Gweon, T. Sasagawa, S. Y. Zhou, J. Graf, H. Takagi, D.-H. Lee, and A. Lanzara, *Nature (London)* **430**, 187 (2004).
 - ⁷ A. Damascelli, Z. Hussain, and Z. X. Shen, *Rev. Mod. Phys.* **75**, 473 (2003).
 - ⁸ A. Lanzara, N. L. Saini, M. Brunelli, F. Natali, A. Bianconi, P. G. Radaelli, and S.-W. Cheong *Phys. Rev. Lett.* **81**, 878 (1998).
 - ⁹ A. J. Millis, P. B. Littlewood, and B. I. Shraiman, *Phys. Rev. Lett.* **74**, 5144 (1995).
 - ¹⁰ F. Masee, S. de Jong, Y. Huang, W. K. Siu, I. Santoso, A. Mans, A. T. Boothroyd, D. Prabhakaran, R. Follath, A. Varykhalov, L. Patthey, M. Shi, J. B. Goedkoop, and M. S. Golden, *Nature Physics* **7**, 978 (2011).
 - ¹¹ A. Taraphder, R. Pandit R., H. R. Krishnamurthy, and T. V. Ramakrishnan, *Int. J. Mod. Phys. B* **10**, 863 (1996).
 - ¹² R. Pankaj and S. Yarlagadda, *Phys. Rev. B* **86**, 035453 (2012).
 - ¹³ E. R. Gagliano, E. Dagotto, A. Moreo, and F. C. Alcaraz, *Phys. Rev. B* **34**, 1677 (1986).
 - ¹⁴ M. E. Fisher, M. N. Barber, and D. Jasnow, *Phys. Rev. A* **8**, 1111 (1973).
 - ¹⁵ S. Datta and S. Yarlagadda, *Solid State Commun.* **150**, 2040 (2010).
 - ¹⁶ We adopt and extend the approach in M. Berciu, *Phys. Rev. Lett* **107**, 246403 (2011).
 - ¹⁷ A. Lenard, *J. Math. Phys.* **5**, 930 (1964).
 - ¹⁸ M. Rigol and A. Muramatsu, *Phys. Rev. A* **72**, 013604 (2005).
 - ¹⁹ S. Reja, S. Yarlagadda, and P. B. Littlewood, *Phys. Rev. B* **86**, 045110 (2012).
 - ²⁰ C. K. Majumdar and D. K. Ghosh, *J. Math. Phys.* **10**, 1388 (1969); C. K. Majumdar, *J. Phys. C: Solid State Phys.* **3**, 911 (1970).
 - ²¹ W.P. Su, J. R. Schrieffer, and A. J. Heeger, *Phys. Rev. Lett.* **42**, 1698 (1979); *Phys. Rev. B* **22**, 2099 (1980).
 - ²² Davide Rossini, Valeria Lante, Alberto Parola and Federico Becca, *Phys. Rev. B* **83**, 155106 (2011).
 - ²³ J. Struck, C. Ölschläger, R. Le Targat, P. Soltan-Panahi, A. Eckardt, M. Lewenstein, P. Windpassinger, and K. Senegstock, *Science* **333**, 996 (2011).
 - ²⁴ T. Mishra, R. V. Pai, S. Mukerjee, and A. Paramekanti *Phys. Rev. B* **87**, 174504 (2013).
 - ²⁵ T. Mishra, R. V. Pai and S. Mukerjee, *Phys. Rev. A* **89**, 013615 (2014).
 - ²⁶ J. Chakhalian, A. J. Millis and J. Rondinelli, *Nature Materials* **11**, 92 (2012).